Formation of silicon triazacorrole and tetrabenzotriazacorrole by the ring contraction of the corresponding tetraazaporphyrin ligands

Nagao Kobayashi,[a,*] Masaki Yokoyama,[a] Atsuya Muranaka[a,b] and Arnout Ceulemans[b]

[a]*Department of Chemistry, Graduate School of Science, Tohoku University, Sendai 980-8578, Japan*
[b]*Division of Quantum Chemistry, University of Leuven, Celestijnenlaan 200F, B-3001 Leuven, Belgium*

Abstract—Silicon-inserted triazacorrole, its μ-oxo dimer, and tetrabenzotriazacorrole have been obtained by ring contraction when metal-free tetraazaporphyrin (TAP) and phthalocyanine (Pc), respectively, were reacted with trichlorohydrosilane ($HSiCl_3$) in the presence of tributylamine in refluxing benzene. The triazacorrole has very sharp absorption at ca. 400 nm, which is suitable for blue-laser applications.

As one of many types of phthalocyanine (Pc) analogue, tetrabenzotriazaporphyrin, in which a *meso*-nitrogen of Pc is replaced by methine-carbon, was reported in the late 1930s.[1,2] Its congener, tetrabenzotriazacorrole (TBC), in which a *meso*-nitrogen of Pc is eliminated to form a direct alpha-C-alpha-C (pyrrole) bond, was suggested in 1986[3] and confirmed by X-ray in 2002.[4] On the other hand, the porphyrin analogue corresponding to TBC, triazacorrole (TAC), was also confirmed for the first time in 2001.[5] Thus the history of TBC and TAC is still young, and there is potential to further explore their chemistry. In this communication, we report the formation of SiTAC **1** (Scheme 1) and SiTBC **3** by ring contraction of tetraazaporphyrin (TAP) and Pc, respectively, observed on silicon insertion to these ligands. In particular, silicon insertion to metal-free TAP (H_2TAP) at higher temperature and prolonged reaction time smoothly and effectively produced SiTAC–O–SiTAC μ-oxo dimer **2** having strong Soret absorption between ca. 360 and 410 nm. This makes it a suitable potential candidate for blue-laser applications.

Commercially available *tert*-butylated H_2TAP (50 mg, 0.093 mmol) was reacted with $HSiCl_3$ (0.2 mL, 2.0 mmol) in the presence of tributylamine (0.3 mL, 1 mmol) in refluxing benzene (10 mL) for ca. 4 h. After removal of the solvent by evaporation, the residue was imposed on an alumina chromatographic column using $CHCl_3$ as an eluent. The fast-eluting pinkish red portion was the μ-oxo dimer **2** (5 mg, 3.6×10^{-3} mmol, 7.7%), the second pink portion was monomer **1**, and a trace amount of SiTAP was also obtained.[6] Since the
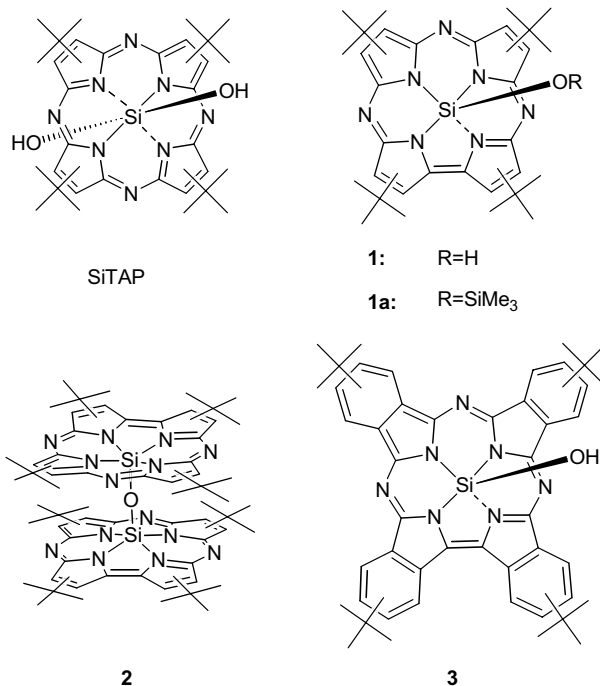
Scheme 1.

purification of **1** was tedious, it was converted to **1a** by reacting trimethylsilylchloride in dry pyridine at 60 °C for ca. 3 h (8 mg, 0.013 mmol, 14% in two steps). If the reaction time in benzene is shortened while keeping the other conditions unchanged, the relative amount of SiTAP and **1** increased compared to the µ-oxo dimer **2**. Thus, shortening the reaction time to ca. 2 h increased the yield of **1** to ca. 40%. On the other hand, prolonging the reaction time to 1–2 day in a small volume of benzene (3 mL) gave **2** in ca. 80–85% yield from the H_2TAP. Commercially available *tert*-butylated H_2Pc was also similarly (4 h, 10 mL of benzene) treated with $HSiCl_3$ in the presence of tributylamine, and gave SiTBC **3** after chromatography, but the yields appeared lower (less than 10%) than the above SiTAP case. Since the same reaction using *tert*-butylated metal-free naphthalocyanine did not give any corresponding triazacorrole product, the ring-contraction reaction appears easier the smaller the starting tetraazaporphyrins.

Figure 1 shows the mass spectra of **1a** and **2** and their theoretical isotopic distribution. The correspondence between the experiments and theoretical distribution is very good, precluding the possibility of other species.

The absorption and magnetic circular dichroism (MCD) spectra of **1a** and **2** are shown in Figure 2. Although the absorption coefficients of the Soret bands of TAP derivatives are generally smaller than those of the Q bands,[7] that of **1a** is characteristic in that it is about twice as large as that of the Q band, and that it is very sharp as that of azaporphyrins. Both the Soret (407 nm) and Q bands (591 nm) appear at shorter wavelengths, and their absorption coefficients (ε(Soret) = 169,500 and ε(Q) = 73,500) per se are smaller than those of a recently reported SiTBC (ε(Soret) = 188,000 at 445 nm and ε(Q) = 120,000 at 668 nm),[4] suggesting that the absorption coefficient increases with increasing size of macrocycle, which is similar to the relationship found between TAPs, Pcs, and naphthalocyanines. The Soret absorption peak of the µ-oxo dimer **2** appeared at a shorter
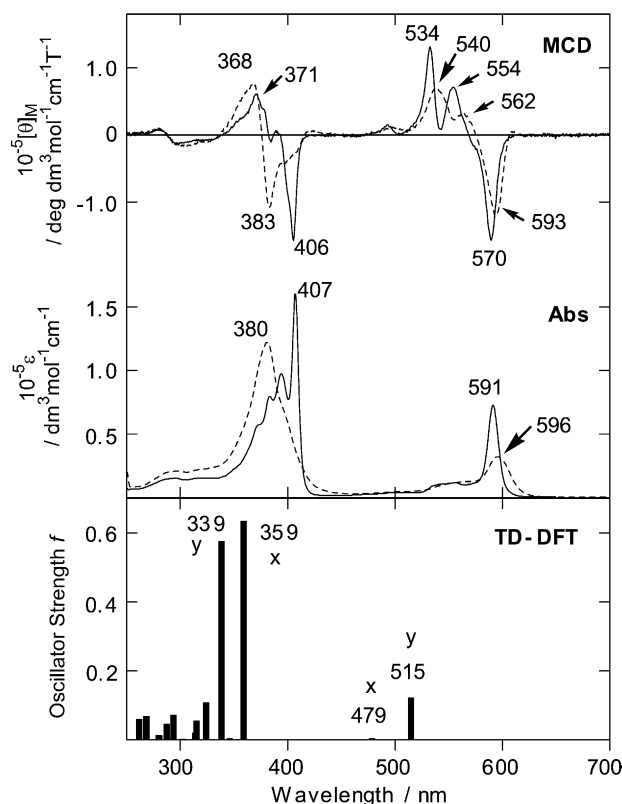
Figure 2. MCD (top) and electronic absorption (middle) spectra of **1a** (solid lines) and **2** (dotted lines) in $CHCl_3$. The calculated electronic absorption spectrum of **1** is shown at the bottom.

wavelength (ca. 360–410 nm) compared to that of monomeric **1**, in accord with the co-facial arrangement[8] of the two chromophores. As has been shown by Pcs, azaporphyrins are more robust than normal porphyrins. Accordingly, SiTAC can be considered a good candidate as dyes for blue-laser applications, although general porphyrins such as octaethyl- and tetraphenylporphyrins have a Soret band in a similar region.
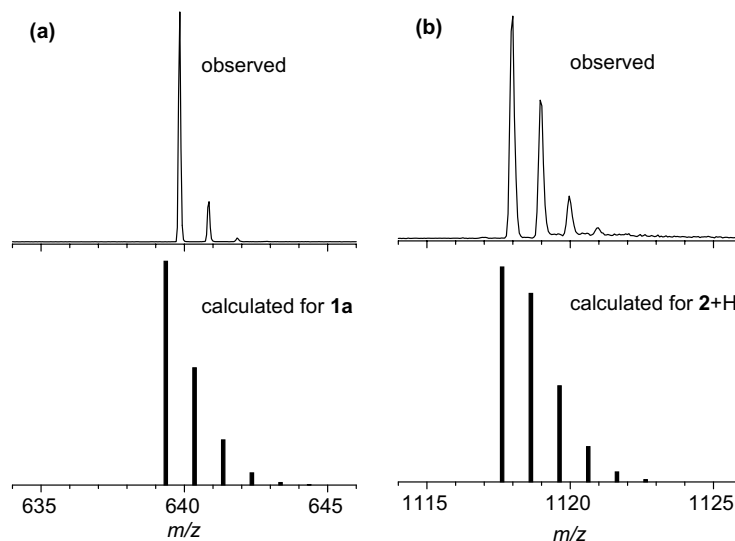
Figure 1. ESI-TOF mass spectra of the molecular ion regions (top) and theoretical isotopic distributions (bottom) for (a) **1a** and (b) **2**.

The MCD spectra of the two compounds are all Faraday B-terms theoretically.[9] Thus, MCD trough and peaks were close to the absorption peaks. In the case of **1**, a negative and positive MCD trough and peak appeared associated with the absorption peak at 591 and 557 nm, indicating that these are two, mutually interacting transitions.[9b,c] From the shape of the MCD, there appear to be at least four transitions in the Soret band region. In the Soret band region of **2**, a dispersion curve between ca. 360 and 390 is a pseudo Faraday A-term produced by two co-facially arranged chromophores, since the MCD of co-facial dimers often does not reflect molecular symmetry of the constituting molecules.[10]

In order to confirm our interpretation of the new compounds, DFT calculations have been carried out for **1** and SiTAP.[11] The peripheral *tert*-butyl groups were omitted and replaced with hydrogen for these calculations. The ground state structures were optimized using C_s (**1**) and C_{2h} (SiTAP) symmetry restrictions.[12] The excitation energies and oscillator strengths were obtained at the density functional level using the time-dependent perturbation theory (TD-DFT) approach.

The accuracy of the optimized structure of **1** can be assessed by comparison with the X-ray crystal structure of the phosphorus TAC derivative reported by Goldberg and co-workers.[5] The optimized corrole framework is almost planar. The distance between the pyrrole α carbon atoms is 1.418 Å, which is very similar to that for the phosphorus complex (1.42(2) Å). In addition, the core sizes of these structures, defined as the distance between the *trans* pyrrole nitrogen atoms, are also very similar (SiTAC **1**: 3.568 Å; P(OMe)$_2$TAC: 3.54 Å).[5]

The calculated electronic absorption spectrum of SiTAC is shown at the bottom of Figure 2, with the calculation results summarized in Table 1. The calculated spectral features appear to be in fairly good agreement with the observed spectrum except for the excitation energies, which are overestimated compared to the experimental values by +0.3 to +0.5 eV. For the Q band region of SiTAC, two weak transitions (Q$_x$ and Q$_y$) are calculated at 479 and 515 nm. Since the polarizations of these transitions are perpendicular to each other, different MCD signs should be observed theoretically.[13] Therefore, the observed weak absorption around 550 and sharp absorption at 591 nm can be assigned to the Q$_x$ and Q$_y$ transitions from the observed MCD patterns. The intense Faraday B term at 534 nm is probably due to the Q$_x$ vibronic band. Similar analyses were applied to the Soret (B) band region. The absorption at 393 and 407 nm were attributed to the calculated intense transitions at 339 (B$_y$) and 359 nm (B$_x$), respectively.

The spectral change from the parent SiTAP to **1** was interpreted on the basis of the Gouterman's four-orbital model[14] because the B and Q transitions for **1** are mainly derived from these orbitals. In the case of SiTAP, both the Q and B bands are nearly doubly degenerate. The intensity and energy of the Q and B transitions change on going from SiTAP to **1** as a result of lowering of molecular symmetry. Figure 3 shows the Gouterman's four orbitals and orbital energies of SiTAP and **1**. The energy of the molecular orbital, which has large coefficients on the *meso*-aza bridges, such as 27b$_u$ orbital of SiTAP, is stabilized due to the higher electronegativity of the nitrogen atoms. By removal of one of the *meso*-aza bridges from the TAP skeleton to form **1**, a distinct destabilization of this kind of molecular orbital occurs: the energy shifts leading to the HOMO−1 (49a′) and LUMO+1 (50a′) of **1** are approximately twice as large as those of the HOMO (39a″) and LUMO (40a″), since the former two orbitals have a large coefficient at the aza bridges, while the latter two orbitals have a nodal plane at the bridges. As a result, the magnitude of the two energy differences, ΔHOMO and ΔLUMO, which represent the energy differences between the two highest occupied π orbitals and the two lowest unoccupied π
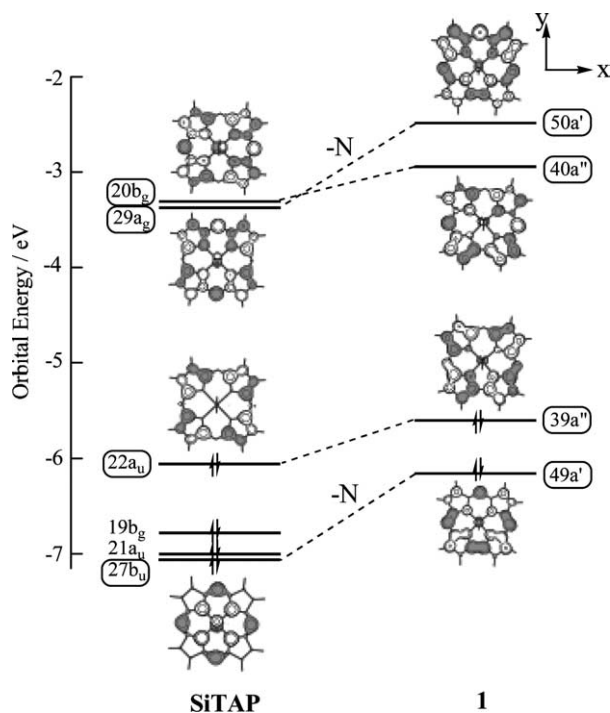

Figure 3. Gouterman's four orbitals and orbital energies of SiTAP and **1**.

Table 1. Selected TD-DFT calculation results of **1**

State	Wavelength (nm)	Energy (cm^{-1})	Assignment	Oscillator strength	Composition (weight, %)	Exp. (nm)
1A′	515	19422	Q$_y$	0.1187	39a″ → 40a″ (80.6); 49a′ → 50a′ (18.5)	591
1A″	479	20895	Q$_x$	0.0033	39a″ → 50a′ (57.4); 49a′ → 40a″ (40.9)	554
2A″	359	27857	B$_x$	0.6052	39a″ → 50a′ (38.1); 49a′ → 40a″ (52.0)	407
3A′	339	29537	B$_y$	0.5499	39a″ → 40a″ (14.4); 49a′ → 50a′ (71.6)	390

orbitals, becomes nearly equivalent ($|\Delta HOMO|$ = 0.56 eV; $|\Delta LUMO|$ = 0.47 eV). This causes a significant mixing of the HOMO+1·LUMO and HOMO−1·LUMO transitions, and consequently cancellation and intensification of the transition dipole moments occurs in the Q_x and B_x bands, respectively. This is similar to typical porphyrin systems.[14] In contrast, the Q_y and B_y bands consist mainly of HOMO·LUMO and HOMO−1·LUMO+1 transitions, which are more similar to typical TAP systems. Indeed the observed Q_x band is much weaker than the B_x band, while the observed Q_y band is rather intense as compared to the Q_x band.

According to Michl's theory,[13] the absolute MCD signs of the four lowest energy electronic transitions of porphyrin derivatives can be correlated with the relative size of $\Delta HOMO$ and $\Delta LUMO$. If $\Delta HOMO > \Delta LUMO$, the sign patterns of MCD band should be −+−+ with increasing energy. The present calculation for **1** suggested $\Delta HOMO > \Delta LUMO$, implying that −+−+ MCD patterns be observed. This prediction agrees well with the observed MCD pattern (Fig. 2).

In summary, we have described silicon triazacorrole and tetrabenzotriazacorrole formation by the ring contraction on silicon-insertion reaction to the metal-free tetraazaporphyrin and phthalocyanine. In the reaction under the same conditions, the corrole formation appears more difficult the larger the starting tetraazamacrocycles. The smallest triazacorrole Si complex and its μ-oxo dimer show strong absorption at around 400 nm, which is potentially suitable for blue-laser applications. The electronic absorption and MCD spectra of silicon triazacorrole have been reasonably interpreted on the basis of DFT calculations.

Acknowledgements

References and notes

1. Barrett, P. A.; Linstead, R. P.; Tuey, G. A. P. *J. Chem. Soc.* **1939**, 1809.
2. Helberger, J. H.; Rebay, A. *Justus Liebigs Ann. Chem.* **1937**, *531*, 279.
3. Fujiki, M.; Tabei, H.; Isa, K. *J. Am. Chem. Soc.* **1986**, *108*, 1532.
4. Kobayashi, N.; Furuya, F.; Yug, G. C.; Wakita, H.; Yokomizo, M.; Ishikawa, N. *Chem. Eur. J.* **2002**, *8*, 1474.
5. Ramdhanie, B.; Stern, C. L.; Goldberg, D. P. *J. Am. Chem. Soc.* **2001**, *123*, 9447; Ramdhanie, B.; Zakharov, L. N.; Rheingold, A. L.; Goldberg, D. P. *Inorg. Chem.* **2002**, *41*, 4105.
6. Selected data of the new compounds. **1a**: ^{1}H NMR (400 MHz, CDCl$_3$) δ 9.11–9.22 (m, 4H, arom), 2.24–2.27 (m, 36H, *t*-Bu), −2.38 (s, 9H, Me). ESI-TOFMS m/z, calcd for C$_{35}$H$_{49}$N$_7$OSi$_2$ [M$^+$] 639.35; found 639.85. **2**: ^{1}H NMR (400 MHz, CDCl$_3$) δ 8.39–9.68 (m, 12H, arom), 1.85 (br s, 36H, *t*-Bu). ESI-TOFMS m/z, calcd for C$_{48}$H$_{49}$N$_7$OSi [M$^+$] 767.38; found 766.96. **3**: ^{1}H NMR (400 MHz, CDCl$_3$) δ 8.37–8.66 (m, 8H, arom), 1.96–2.38 (m, 72H, *t*-Bu). ESI-TOFMS m/z, calcd for C$_{64}$H$_{80}$N$_{14}$OSi$_2$ [M$^+$+H] 1117.63; found 1118.00. SiTAP: ^{1}H NMR (400 MHz, CDCl$_3$) δ 9.02–9.12 (m, 4H, arom), 2.23–2.26 (m, 36H, *t*-Bu). ESI-TOFMS m/z, calcd for C$_{32}$H$_{42}$N$_8$O$_2$Si [M$^+$−2OH+CH$_3$O] 595.33; found 595.35.
7. (a) Luk'yanets, E. A. *Electronic Spectra of Phthalocyanines and Related Compounds*; NIOPIK: Moscow, 1989; (b) Kobayashi, N. In *Phthalocyanines—Properties and Applications*; Leznoff, C. C., Lever, A. B. P., Eds.; VCH: New York, 1993; Vol. 2, Chapter 3; (c) Kobayashi, N. In *Porphyrin Handbook*; Kadish, K. M., Smith, K. M., Guilard, M., Eds.; Elsevier Science: New York, 2003; Vol. 15, Chapter 100.
8. (a) Kobayashi, N.; Lever, A. B. P. *J. Am. Chem. Soc.* **1987**, *109*, 7433; (b) However, the red-shift of the Q band is unexpected.
9. (a) Stillman, M. J.; Nyokong, T. In *Phthalocyanines— Properties and Applications*; Leznoff, C. C., Lever, A. B. P., Eds.; VCH: New York, 1989; Vol. 1, Chapter 3; (b) Tajiri, A.; Winkler, J. *Z. Naturforsch.* **1983**, *38a*, 1263; (c) Kaito, A.; Nozawa, T.; Yamamoto, T.; Hatano, M.; Orii, Y. *Chem. Phys. Lett.* **1977**, *52*, 154.
10. Kobayashi, N.; Togashi, M.; Osa, T.; Ishii, K.; Yamauchi, S.; Hino, H. *J. Am. Chem. Soc.* **1996**, *118*, 1073.
11. All calculations have been carried out at the DFT level using the B3-LYP hybrid functional as implemented in TURBOMOLE.[15] Def-SV(P) basis sets were used for the geometry optimizations of the ground states. The excitation energies and oscillator strengths have been obtained at the density functional level using the time-dependent perturbation approach (TD-DFT) with TZVP basis sets. The analysis of the electronic structure in this study is based on the Kohn–Sham molecular orbitals generated by the DFT method: analogous LCAO-MOs were obtained with the Hartree–Fock formalism.
12. SiTAP contains two hydroxy groups as axial ligands, and it appears reasonable to assume that the Si atom is in the TAP plane. Taking the HO–Si–OH structure into consideration, the ground state structure of SiTAP was optimized using C_{2h} symmetry restrictions.
13. Michl, J. *J. Am. Chem. Soc.* **1978**, *100*, 6801, 6812.
14. Gouterman, M. In *The Porphyrins*; Dolphin, D., Ed.; Academic: New York, 1978; Vol. 3, Chapter 1.
15. Ahlrichs, R.; Bär, M.; Baron, H.-P.; Bauernschmitt, R.; Böcker, S.; Ehrig, M.; Eichkorn, K.; Elliot, S.; Haase, F.; Häser, M.; Horn, H.; Huber, C.; Huniar, U.; Kattannek, M.; Kölmel, C.; Kollwitz, M.; Ochsenfeld, C.; Öhm, H.; Schäfer, A.; Schneider, U.; Treutler, O.; von Arnim, M.; Weigend, F.; Weis, P.; Weiss, H. *TURBOMOLE*; University of Karlsruhe: Karlsruhe, Germany, 2002; Version 5.6.